JOURNAL OF APPLIED ELECTROCHEMISTRY **29** (1999) 51–57

Influence of structural parameters on the properties of electrolytic Ni–Mn–S deposits

N. ATANASSOV

Institute of Physical Chemistry, Bulgarian Academy of Sciences, 1113 Sofia, Bulgaria
E-mail: atanasso@ipchp.ipc.acad.bg

H. W. SCHILS

Forschungsinstitut für Edelmetalle und Metallchemie, 73525 Schwäbisch Gmünd, Germany

Received 19 March 1997; accepted in revised form 10 February 1998

Microstructural parameters such as coherent domain size, microstrain, dislocation density and texture of electrolytically plated Ni–Mn–S layers were investigated by X-ray analysis. Structural parameters, layer composition and the macroproperties are discussed and explained. With the help of a statistical regression analysis the correlation coefficient r^2 and its relationship with the investigated parameters is determined. It is shown that the microstructural parameters play an important role in determining the macroscopic properties. The manganese concentration is shown to influence the structural parameters, but no influence of sulphur is found. It seems that a relationship of the structural parameters with the macroscopic properties is valid in general and is not a special case. There structural correlations can be used in general for processing electrolytic deposits for required applications.

Keywords: *codeposition Ni, Mn, S, X-ray analysis*; *structure*; *texture*; *properties*

1. Introduction

The effect of manganese on the electrocrystallization mechanism of nickel deposits was reported earlier [1, 2]. Sulfamate electrolytes were used and it was found that manganese plays an important role in the incorporation of S, C, H and O in the deposits. By varying the parameters in pulse plating studies, the effects of the individual factors responsible for the incorporation of manganese were investigated. It is known that deposition of manganese takes place at a strongly negative potential (−1.18 V), making the simultaneous deposition of both Ni and Mn difficult. It was assumed that the incorporation of manganese does not take place by typical electrochemical metal ion transfer but probably due to a specific surface reaction occurring at the hydrogen-saturated Ni-cathode [2, 3].

Our interest in studying the role of manganese on the electrolytic deposition of nickel arose through reported results from several authors [3–5], who showed that the incorporated manganese had a positive effect on the physical and mechanical properties of heat-treated nickel films such as tensile strength, yield point, ductility and microhardness. The authors concluded, that sulphur was the main factor causing embrittlement in the deposits and that a certain amount of Mn (Mn : S = 25 : 1 [4] or 5 : 1 [5]) is necessary to avoid sulphur-embrittlement. Because of its large affinity, manganese reacts at elevated temperatures with sulphur and the migration of sulphur towards the grain-boundaries is inhibited. After heat treatment, we agree with the other authors that NiS layers without manganese develop sulphur embrittlement. Sulphur was incorporated in the deposits by addition of CHT (2,4-dichloro-5-sulfamoylbenzoic acid) [6] to the electrolyte. The NiS-deposits maintain excellent properties below 260 °C such as microhardness, wear-resistance, internal stress and ductility [7, 8].

Later the morphology and texture of the deposits were investigated [9, 10]. The texture, which is especially sensitive to any change in the deposit, can be regarded as one of the most important structural parameters in describing the state of the deposit. The texture index TI describing the degree of preferred orientation in the deposits was used. A possible relation between texture index, composition, structural parameters and macroproperties of the plated films was investigated. It was shown that the texture index can be used as a criterion in predicting material properties [9]. The investigation also showed that recrystallisation rate was dependent on initial texture parameters, probably together with other structural parameters, a finding which is essential with regard to the microhardness and ductility within a wide temperature range.

So far methods of investigation using microstructural characteristics to predict the mechanical and physical behaviour of an electroplated material have

© 1999 Kluwer Academic Publishers.

hardly been used. Such methods are necessary for a quantitative description of the microstructure in order to predict macroscopic properties. Only recently the X-ray diffraction technique has been used [11, 12]. Many material properties are anisotropic and are influenced by the crystal-orientation in the material. Some of these properties are Young's modulus, the electrical conductivity and the magnetic permeability. The most important parameter in describing the anisotropy is the texture [13], which describes the preferred orientation of crystallites in a given material and at the same time the deviation from a statistically random structure.

The investigation of structural parameters, the elemental- and phase-analysis of the Ni–Mn–S deposits makes it possible to answer the questions about the final macroscopic properties of a given deposit. Sulphur embrittlement is only a specific part of the recrystallization process, which occurs at high temperatures in Ni-based materials. It is, therefore, important to determine the factors influencing of the rate and degree of the recrystallization, which deteriorate the mechanical and technological properties of the material. The objective of this paper is to discuss the influences of structural parameters on deposition parameters and the role of each plating parameter in determining the final properties of the deposits. Control of the plating process to the specific demands on the deposits then becomes feasible.

2. Experimental details

Thin foils of 5 nm thickness were electroplated using a conventional nickel sulfamate electgrolytic bath: 80 g dm^{-3} nickel, 35 g dm^{-3} boric acid, 3 g dm^{-3} $NiCl_2$. 5 g dm^{-3} manganese in the form of mangaese sulfamate or manganese chloride and either 0.1 or 0.4 g dm^{-3} of the sulphur–containing substance CHT (2, 4-dichloro-5-sulfamoylbenzoic acid) [6] were added. The deposits were produced with direct current and pulsed current parameters were: 10 ms pulse duration, switch time 0.2–5 ms, duty cycle Θ from 2 to 50%, mean current density (D_k) 1–5 A dm^{-2} and pulse current density (I_p) from 10 to 50 A dm^{-2}. The manganese content was measured with AAS, sulphur was estimated by combustion in oxygen (Leco CS 225), the Vickershardness ($HV_{0,1}$) was measured with a load of 100 g with Durimet 2 (equipment from Leitz), the ductility with a mechanical bulge tester (ball diameter 8 mm, rate 440 mm s^{-1}) according to DIN 50102 specifications.

The X-ray investigations were made with a Siemens D-5000 diffractometer equipped with an open asymmetric Eulerian cradle for measuring stress and texture. Measurements for the profile analysis were made using (θ–2θ) Bragg–Brentano geometry and a focussed symmetric CuK_α radiation beam. The step width used was 0.02° in 2θ. The measuring times were dependent on the intensity of the (2 0 0)-interference and ranged from 12 to 28 s per step. A Ni film was used as standard, deposited electrolytically from a sulfamate bath without additives after heat treatment for 2 h at 690 °C [14]. The X-ray texture analysis of the electroplated Ni–Mn–S deposits were carried out using the Schulz technique [15]. The pole figures of the lattice-planes (1 1 1), (2 0 0) and (2 2 0) were measured in the range $\chi \leq 75°$.

3. Method and interpretation of the X-ray results

The X-ray diffraction line profile analysis is a method for characterizing the microstructure in polycrystalline materials. Both small domain sizes, coherent scattering regions, and variable lattice strains lead to a broadening of the interference lines [16–19]. For the structural investigations it was assumed that the deposits were homogeneous, but practically these deposits are nonhomogeneous and the average values of the defect density were determined. The Ni–Mn–S deposits were investigated by the Voigt method [20–22]. This is a single line analysis, which allows quick calculation of the microstructural data with only one line profile of the deposit and one line profile from a standard probe. The physical, true profile f is determined with the typical parameters of the broadened profile h and the standard profile g. These parameters were calculated after approximation of the profiles with a Voigt function, which is a convolution of Cauchy and Gauss functions. Domain size broadening tends to give a Cauchy line and microstrain broadening produces a Gaussian line. By mathematical means, the integral width value can be split into Gauss- and Cauchy parts calculated for the physically true profile f of the sample. From the integral width of the Cauchy part (index C) in profile f, the domain size D is calculated as

$$D = \frac{\lambda}{\beta_{Cf} \cos\theta} \tag{1}$$

where λ is the wavelength of the used X-ray radiation and θ is the Bragg angle.

The integral width of the Gaussian part (index G) of the profile f gives a measure of the microstrain:

$$\langle \varepsilon^2 \rangle^{1/2} = \frac{\beta_{Gf}}{4 \tan\theta} \tag{2}$$

With the knowledge of $\langle \varepsilon^2 \rangle^{1/2}$ and D [10, 23, 24] the dislocation densities of polycrystalline metals can be estimated using the relation

$$\rho = \frac{k}{b} \frac{\langle \varepsilon^2 \rangle^{1/2}}{D} \tag{3}$$

where $k = 2\sqrt{3}$ and b is the Burger's vector.

The estimation of dislocation densities in electrolytic deposits is, however, still a practical problem with great difficulties, because the influence of grain boundaries and incorporated atoms (manganese and sulphur) on the microstrain cannot be neglected. Possible interpretation is to characterize the ratio $\langle \varepsilon^2 \rangle^{1/2}/D$ as growth limiting defects.

In Table 1 the electrolytic conditions are listed: the kind of current density (d.c. or pulse current), the

Table 1. Deposition conditions, layer composition and line profile values of the Ni–Mn–S layers

Sample	*Electrolytic conditions*				*Layer composition*		*Line profile values*		
	D_k /A dm^{-2}	*DC*	*Ip* /A dm^{-2}	*CHT* /g dm^{-3}	*S* /ppm	*Mn* /%	β	*2w*	$2w/\beta$
1	5.0	DC		0.4	510	0.61	1.0850	0.7995	0.7369
2	5.0		50	0.1	200	0.37	0.9243	0.6644	0.7188
3	5.0		50	0.4	400	0.53	1.0235	0.7626	0.7451
4	2.5		50	0.4	290	0.44	0.9974	0.7465	0.7484
5	5.0		50	0.4	320	0.46	0.9468	0.7112	0.7512
6	5.0		10	0.4	340	0.39	0.9099	0.6871	0.7551
7	2.5		50	0.4	250	0.31	0.8975	0.6812	0.7590
8	5.0	DC		0.4	600	0.45	0.8319	0.6320	0.7597
9	1.0		50	0.4	280	0.11	0.5876	0.4589	0.7810
10	2.5		50	0.1	180	0.18	0.5302	0.4146	0.7820
11	5.0	DC		0.1	230	0.23	0.5311	0.4236	0.7976
12	1.0		10	0.4	240	0.09	0.5100	0.4062	0.7965
13	1.0		50	0.4	280	0.10	0.4772	0.3830	0.8026
14	2.5	DC		0.1	150	0.14	0.4517	0.3612	0.7996
15	1.0		50	0.1	140	0.08	0.4368	0.3541	0.8107

mean current density D_k, the pulse current density I_p, and the concentration of the sulphur containing addition CHT. Also listed are the most important compounds of the layer composition, the amounts of manganese and sulphur incorporated, and the characteristic values of the X-ray analysis as the halfwidth $2w$ and β and their ratio $2w/\beta$. The amount of manganese incorporated varies from 0.08 to 0.61%, although the amount of manganese in the electrolyte is always 5 g dm^{-3}.

The upper part of Table 1 lists samples, plated with higher d.c. current and higher pulse current density. In samples of this kind, a larger amount of both manganese and sulphur is incorporated due to the higher overvoltage. These samples have a larger line width than the second group (nearly a factor of two), but the ratio $2w/\beta$ does not differ much. These values fluctuate midway between a Cauchy and a Gaussian distribution. This distribution shows that the line broadening caused by domain size and microstrain is nearly the same for both groups. A tendency of domain-size-broadening for the upper group is favoured only slightly.

A full interpretation and mapping of potential correlations between various parameters is not simple. Therefore, we have chosen a statistical method, which makes it possible, by regression analysis, to analyse the relations among the measured parameters. Correlation between individual factors is described by the method of least squares. This means that for a linear dependence all the points investigated lie on a regressional straight line. The correlation coefficient r^2 is 1 in this case. The correlation coefficient r^2 becomes small with the scatter of the data points from the regression straight line. For practical purposes in these complex materials and many seemingly diverse parameters, a correlation coefficient r^2 higher than 0.8 represents a strong correlation. According to Fig. 1 there exists an unambiguous relation between the half-intensity peak width (Table 1) and the previously measured microhardnesses [1].

The investigated Ni–Mn–S deposits show $\langle 1\,0\,0\rangle$ fibre texture (Fig. 2), which is often accompanied by a $\langle 2\,2\,1\rangle$-twin texture (Table 2) [25–28]. In one single case, a $\langle 1\,1\,0\rangle$ fibre texture was observed. The Table presents the texture positions as well as the pole densities of the experimental pole figures. The accompanying texture index TI describes the sharpness of the texture, without regard to the individual distributed orientations. In the case of nonsystematic distribution, the TI value is 1 and for a perfect single crystal the value is unlimited [9, 28]. An evaluation of the preferred orientation is simplified by the fact that practically all the samples contain $\langle 1\,0\,0\rangle$ texture. The texture index of the investigated Ni–Mn–S deposits varies from 1.11 to 8.16 with an almost random crystal distribution (1.11) and a very sharp fibre texture (8.16), compared to most electrolytic deposits.

4. Results and discussion

In Table 3, three different groups of parameters are presented. The first group concerns the composition of the deposits, the second the structural parameters

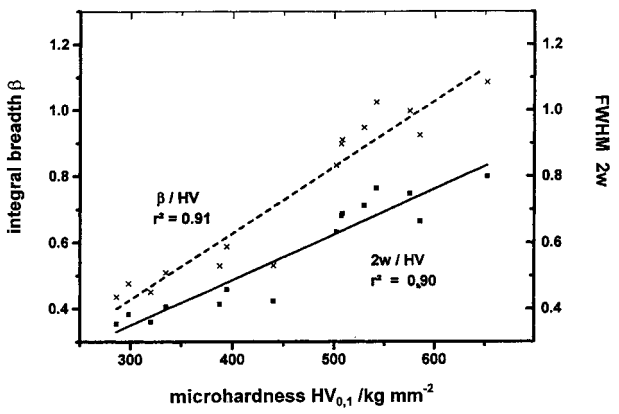

Fig. 1. Relationship between microhardness HV and 2w (full width at half maximum) and β (integral breadth).

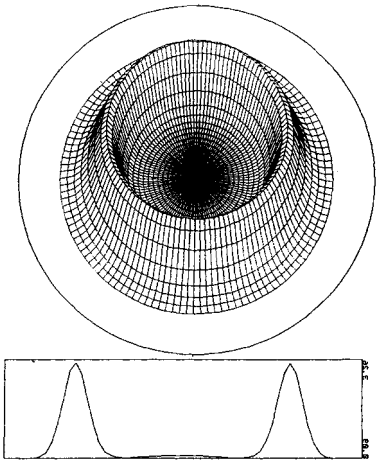

Fig. 2. The (1 1 1) pole figure of sample 12 shows a typical (1 0 0) fibre texture: (a) The 3D-(1 1 1) pole figure; (b) intensity against angle ψ of the (1 1 1) pole figure.

and the third presents the macroscopic properties. As can be seen from Table 3, the amounts of Mn and S incorporated in the layers vary within wide ranges. The sulphur concentration lies between 140 and 600 ppm, and is related to the CHT-concentration in the plating electrolyte. At low CHT concentration ($0.1\,g\,dm^{-3}$), the sulphur content lies in the range of 140 to 230 ppm. At higher CHT concentration ($0.4\,g\,dm^{-3}$), 240 to 600 ppm of sulphur is incorporated in the deposits. Similarly, the Mn content shows a large variation from 0.08 to 0.61%. In this case the Mn concentration is related to the mean current (D_k) and pulse current (I_p) densities during plating. Higher current densities lead to a higher Mn content in the deposits. Obviously this is caused by the lowering of plating-potential to a value nearer to the deposition potential of Mn. Large variations of the domain size, structural defect and the degree of preferred orientation are observed in the structural parameters. Even though it is not an easy task to estimate the deposition-overpotential for pulse-plating, there exists a clear tendency towards decreasing domain size with increasing D_k and I_p as well as overpotential.

From Table 3 two types of deposit are clear. One is characterized by high values of structural defect parameters such as microstrain and dislocation density. These deposits possess higher microhardness, smaller domain size and lower value of texture index. In the second group, the deposits have fewer structural defects, larger domain size, and higher value of texture index. A central question is: 'How strong is the relationship among the parameters, such as electrolytic conditions, layer composition, structural parameters, and macroscopic properties'?

It is likely that both the Mn concentration and the deposition conditions (overpotential, values of D_k and I_p) affect the separation into the two groups. At present it is difficult to say whether the higher values of the overpotential (which shifts the deposition potential in the direction of manganese deposition) is the only cause of the large content of the Mn in the layer. The other possibility is the large amount of hydrogen development at the cathode. The hydrogen development lowers the barrier potential to Mn deposition [2, 3].

For a detailed analysis of the experimental data, the statistical regression analysis was used. Table 4 shows the linear correlation coefficients r^2 of the different groups of parameters, such as layer composition, structural parameters and the mechanical properties. Here it is possible, on one hand, to examine the influence of layer composition on the structural parameters and, on the other hand, the mechanical properties and to separate and quantify the influence of the structural parameters on the mechanical properties.

The results clearly show correlations among the deposited Mn content on the microstrain ε (Fig. 3) and on the dislocation density ρ (Fig. 4). The deposition of foreign atoms occurs dominantly in the grain boundaries and, therefore, the results of the dislocation density ρ can be considered as growth limiting defects.

The influence of Mn on domain size ($r^2 = 0.78$) and texture index (TI) ($r^2 = 0.74$) cannot be easily interpreted. The current parameters D_k and I_p influ-

Table 2. Texture components of the Ni–Mn–S layers

Sample	*Preferred orientation*	*Texture index*	*Pole density*		
			⟨2 0 0⟩	⟨1 1 1⟩	⟨2 2 0⟩
1	⟨1 0 0 + 2 2 1⟩	1.17	2.3	1.3	1.1
2	⟨1 1 0⟩	1.11	1.2	1.2	1.5
3	⟨1 0 0 + 2 2 1⟩	1.27	2.8	1.4	1.3
4	⟨1 0 0 + 2 2 1⟩	1.49	3.8	1.6	1.4
5	⟨1 0 0 + 2 2 1⟩	1.50	3.9	1.8	1.4
6	⟨1 0 0 + 2 2 1⟩	2.11	6.2	2.2	1.6
7	⟨1 0 0 + 2 2 1⟩	2.10	5.9	1.9	1.6
8	⟨1 0 0 + 2 2 1⟩	2.43	7.2	2.3	1.7
9	⟨1 0 0 + 2 2 1⟩	4.03	11.5	2.8	2.0
10	⟨1 0 0 + 2 2 1⟩	4.13	11.6	2.9	2.0
11	⟨1 0 0⟩	3.17	9.7	2.5	1.8
12	⟨1 0 0⟩	4.71	12.3	3.0	2.0
13	⟨1 0 0⟩	6.09	15.0	3.0	2.3
14	⟨1 0 0⟩	6.95	18.8	3.8	2.5

Table 3. Layer composition, structural parameters and mechanical properties of the Ni–Mn–S layers

Sample	*Layer composition*		*Structural parameters*				*Mechanical properties*	
	S /ppm	*Mn* /%	*Texture index*	*D* /nm	10^3_ε /%	10^{10}_ρ /cm^{-2}	$HV_{0,1}$ /kg mm^{-2}	*Dct* /%
1	510	0.61	1.17	14.1	4.36	31	650	1.6
2	200	0.37	1.11	15.5	3.11	20	585	0.9
3	400	0.53	1.27	15.7	4.30	27	542	2.2
4	290	0.44	1.49	16.4	4.26	26	575	2.7
5	320	0.46	1.50	17.7	4.07	23	530	1.3
6	340	0.39	2.11	18.9	3.98	21	508	2.0
7	250	0.31	2.10	19.6	4.01	20	507	2.2
8	600	0.45	2.43	21.4	3.67	17	502	2.8
9	280	0.11	4.03	37.3	2.63	7	394	2.3
10	180	0.18	4.13	42.8	2.27	5	387	4.5
11	230	0.23	3.17	48.5	2.51	5	440	4.5
12	240	0.09	4.71	50.7	2.34	5	335	4.0
13	280	0.10	6.09	58.8	2.19	4	298	6.1
14	150	0.14	6.95	61.8	1.95	3	320	7.3
15	140	0.08	8.16	72.4	1.98	3	286	3.3

ence the incorporation of Mn and the domain size, and gives an indirect correlation between them. A similar explanation may be given for the correlation between the Mn content and texture index of the layers. Larger domains have a higher degree of orientation and stronger TI [9]; this is verified by higher values of r^2.

The influence of incorporated Mn on microhardness has been reported [3, 29]. The correlation between incorporated Mn and microhardness found from our data ($r^2 = 0.87$) confirms this quantitatively.

In the case of sulphur, a different situation exists. As seen from Table 4, no direct correlation exists between the amount of incorporated sulphur and the other parameters. This finding is surprising, because this is not reported in the literature.

The obtained linear correlation between Mn and ρ is a synonymous proof of the influence of Mn on the structure, while the low values of r^2 in respect to the amount of incorporated sulphur show that it is not able to play such role on the structure. An direct influence of S-containing CHT additive, may exist on the rate and mechanism of electrochemical processes, on which the structural parameters of the layers also depends.

The influence of the current conditions, alloy components and the structural parameters on the ductility cannot be clearly interpreted. The content of the incorporated alloy components, sulphur ($r^2 = 0.17$) and manganese ($r^2 = 0.43$) has no linear relationship with the ductility.

Nevertheless, as it seen in Table 3, there is an apparent tendency for an increase in ductility with decrease in Mn and S amount. This can be related to the weaker incorporation in grain bondaries.

It is not surprising that structural parameters do not have a linear relationship with ductility, and the correlation coefficient values r^2 vary between 0.53 to 0.62. For experimental ductility data, the measuring conditions, film thickness and macrodefects, such as cracks and pores, are important.

In contrast, microhardness is not so dependent on the distribution of alloy components in the grain volume and the grain boundaries. In this case, an unambigous correlation between different parameters and this important macroscopic property occurs. The r^2 values range from 0.80 to 0.89. For example, the relationship between the microhardness and crystallite size with a r^2 value of 0.89 is clearly shown in Fig. 5. The results suggest that the domain size has a

Table 4. Correlation coefficients r^2 between the mechanical properties, structural parameters and contents of S and Mn

	Layer composition		*Structural parameters*				*Mechanical properties*	
	S	*Mn*	*TI*	*D*	ε	ρ	*HV*	*Dct*
S	–	0.52	0.33	0.37	0.44	0.38	0.33	0.17
Mn	0.52	–	0.74	0.78	0.85	0.90	0.87	0.43
TI	0.33	0.74	–	0.94	0.77	0.75	0.88	0.55
D	0.37	0.78	0.94	–	0.85	0.85	0.89	0.62
ε	0.44	0.85	0.77	0.85	–	0.94	0.80	0.53
ρ	0.38	0.90	0.75	0.85	0.94	–	0.88	0.56
HV	0.33	0.87	0.88	0.89	0.80	0.88	–	0.58

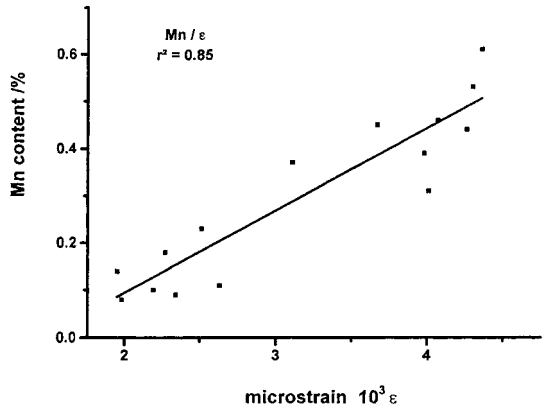

Fig. 3. Relationship between the Mn content and the microstrain ε.

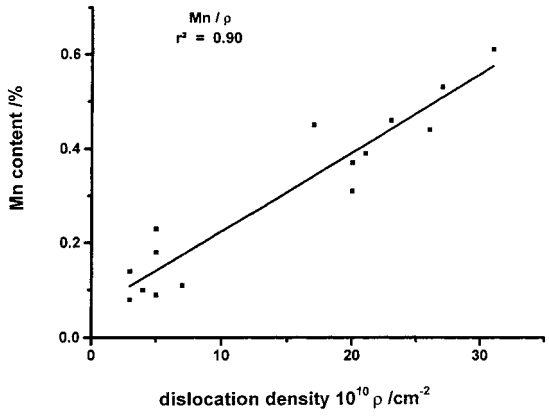

Fig. 4. Relationship between the Mn content and the dislocation density ρ.

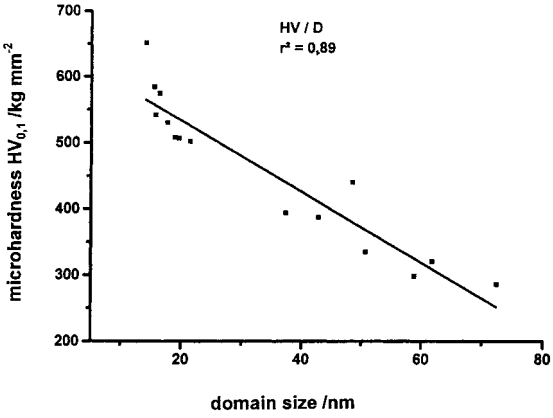

Fig. 5. Relationship between the microhardness HV and the domain size D.

lower limit of about 14 nm, corresponding to a maximum hardness of 650 kg mm^{-2}.

The statistical data show that all the structural parameters are related to one another (Table 4). The large influence of the TI on D ($r^2 = 0.94$) is evident, while the influence of TI on ε ($r^2 = 0.77$) and on ρ ($r^2 = 0.75$) is not so well established, but is still a fact. The r^2 values of the other structural parameters, as calculated from the line broadening from the X-ray diffraction lines, vary from 0.85 to 0.94 and

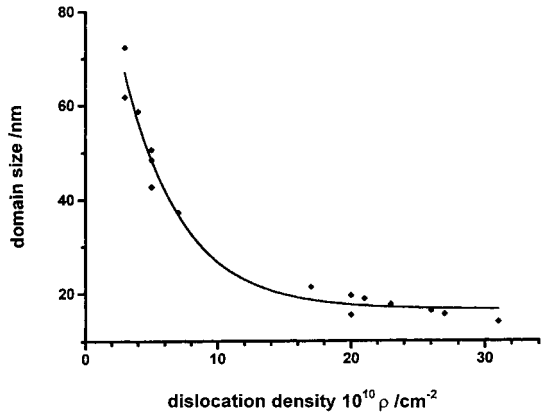

Fig. 6. Relationship between the domain size D and the dislocation density ρ.

confirm the inter-relationship of all structural parameters. The relationship between the domain size and dislocation density ρ is very interesting. In spite of the high value of the linear correlation between these characteristics, Fig. 6 shows the presence of two clearly delineated regions with different slopes. It can therefore by assumed that the influence of additional factor, the amount of incorporated Mn, is significant. At low values of Mn ($<0.2\%$) ρ decreases relatively despite the unexpected jump in domain size. In the second region of the relationship, where Mn is present in large amounts, small changes in D (14–21 nm) cause a rapid increase in dislocation density, ρ.

These results show a complex influence of different factors. These factors can influence the formation of Ni–Mn–S layers with determinate characteristics in different ways.

Acknowledgement

The authors are grateful to the Deutsche Forschungsgemeinschaft, Bonn, and National Sciences Fund of Bulgaria, Sofia, for their financial support of this joint project.

References

[1] N. Atanassov, U. Heuberger and Ch. Raub, *Metalloberfläche* **46** (10) (1992) 448.
[2] N. Atanassov and W. Mitreva, *Surf. Coat. Technol.* **78** (1996) 144.
[3] G. A. Malone, *Plat. Surf. Finish.* **74** (1987) 50.
[4] J. W. Dini, H. R. Johnson and L. A. West, *Plat. Surf. Finish.* **65** (1978) 36.
[5] W. R. Wearmothh and K. C. Belt, *ibid.* **66** (1979) 53.
[6] *US Patent 4 585 531* (1986), *Bulgarian Patent 54 663* (1981).
[7] N. Atanassov and A. Sofianska, *Galvanotechnik* **79**(5) (1988) 1485.
[8] N. Atanassov, A. Sofianska and W. Mircheva, *ibid.* **84**(6) (1993) 1879.
[9] H. W. Schils and N. Atanassov, *Trans. Inst. Met. Finish.* **73** (1995) 37.
[10] N. Atanassov and H. W. Schils, *Plat. Surf. Finish.* **83**(7) (1996) 49.
[11] G. K. Williamson and R. E. Smallman , *Phil. Mag.* **1** (1956) 34.
[12] B. E. Warren, *Progress in Metal Physics* **8** (1959) 147.
[13] H. J. Bunge, Z. *Metallkunde* **75** (1984) 97.

[14] U. Wolfstieg and E. Macherauch, 'Eigenspannungen', DGM-Inf., Oberursel (1979), p. 345.
[15] L. G. Schulz, *J. Appl. Phys.* **20** (1949) 1030.
[16] W. H. Hall, *Proc. Phys. Soc.* A **62** (1949) 741.
[17] G. K. Williamson and W. H. Hall, *Acta. Metall.* **1** (1953) 22.
[18] B. E. Warren and B. L. Awerbach, *J. Appl. Phys.* **21** (1950) 595.
[19] P. Klimanek, *Freiberger Forschungsheft* B **132** (1968) 76.
[20] J. I. Langford, *J. Appl. Cryst.* **11** (1978) 10.
[21] Th. H. De Keijser, J. I. Langford, E. J. Mittemeijer and A. B. P. Vogels, *ibid.* **5** (1982) 308.
[22] R. Delhez, Th. H. De Keijser and E. J. Mittemeijer: *Fresenius' Z. Phys. Chem.* **312** (1982) 1.
[23] D. E. Mikkola and J. B. Cohen, *Proc. Met. Soc. Conf.* **36** NY (1965) 289.
[24] F. Burgahn, O. Vöhringer and E. Macherauch, *Z. Metallkunde* **84** (1993) 224.
[25] G. Wassermann and J. Grewen, 'Texturen Metallischer Werkstoffe', Springer Verlag, Berlin (1962).
[26] N. Pangarov and I. Tomov, *Izw. otd. Khim. nauki* **2** (1969) 819.
[27] I. Tomov and H. J. Bunge, *Texture Cryst. Solids* **3** (1979) 73.
[28] H. J. Bunge, 'Texture Analysis in Materials Science', Butterworths, London (1982).
[29] W. B. Stephenson, *Plating* **53** (1966) 183.